Electronic Supplementary Information for

Three Dimensional Porous Hofmann Clathrate $[M^{II}Pt^{II}(CN)_4]_\infty$ (M = Co, Ni) Synthesized by Using Postsynthetic Reductive Elimination

Takuro Okamora,[a] Bin Wu, [ab] Hiroaki Iguchi,[a] Brian K. Breedlove,[a] Masahiro Yamashita,[abd] Wataru Kosaka,[c] Hitoshi Miyasaka,[c] Shinya Takaishi, *,[a]

[a]Department of Chemistry, Graduate School of Science, Tohoku University, 6-3 Aza-aoba, Aramaki, Sendai 980-8578, Japan

[b]Advanced Institute for Materials Research, Tohoku University, 2-1-1 Katahira, Sendai 980-8577, Japan

[c]Institute for Materials Research, Tohoku University, 2-1-1 Katahira, Sendai 980-8577, Japan

[d]School of Materials Science and Engineering, Nankai University, Tianjin 300350, China.

Contents

I. Materials.

K_2PtCl_4 was obtained by Mitsuwa Chemicals Co., Ltd, and used as received. KCN, $AgNO_3$, $Co(NO_3)_2 \cdot 6H_2O$, $NiBr \cdot 3H_2O$, and Br_2 were obtained by Wako Pure Chemical Industries, Ltd, and used as received.

II. Characterization and Instrumental Procedures

Single-crystal X-ray diffraction collected on Bruker APEX-II diffractometer with an APEX II CCD detector and JAPAN thermal Engineering Co., Ltd Cryo system DX-CS190LD. N_2 isotherm at 77 K was performed using microtrac Bell sorp Max. Thermogravimetric analysis was performed using Shimadzu DTG-60H under a N_2 gas flow (50 ml/min) or areobic condition with a sweep rate of 1 K/min unless otherwise noted. Powder X-ray diffraction (PXRD) of **1**, **1"**, **2**, and **2"** were measured in air (θ–2θ scan) using Bruker PHASER diffractometer with Cu Kα radiation source. PXRD of **1'** and **2'** were measured in dry N_2 atmosphere (transmission geometry with a sealed capillary) using Rigaku RINT2000 diffractometer. Magnetic susceptibilitis were measured using Quantum Design MPMS-5 SQUID magnetometer under 1000 Oe DC field. UV-Vis-NIR spectra were measured using Shimadzu UV-3100PC spectrometer with an integrating sphere unit. Diffuse reflectance spectra were transformed to absorbance spectra using Kubelka-Munk function. FT-IR spectra were measured using Jasco FT-IR 4200 spectrometer with ATR unit. ICP-OES measurements were performed in Shimadzu ICPE-9000 installed at the research and analytical center for giant molecules in Tohoku university. Emissions at 228.616(1), 231.604(1) and 214.423(1) nm are used for Co, Ni and Pt elements, respectively.

III. Syntheses

Synthesis of 1

To 5 ml of aqueous solution of K_2PtCl_4 415 mg (1.00 mmol) was added KCN 260 mg (4.00 mmol) and stirred until the solution became colorless. $AgNO_3$ 679 mg (4.00 mmol) was added and stirred ca. 24 h under dark. The precipitate (AgCl) was filtered off by celite filtration. Approximately 250 mg (~1.5 eq) of Br_2 was added and stirred for 30 min, and then heated to 50 °C for another 30 min to remove excess of Br_2 in the solution. After cooling, to the solution was added 5 ml of 0.2 M aqueous solution of $Co(NO_3)_2 \cdot 6H_2O$ and stand overnight. Obtained orange color crystals of $[Co(H_2O)_2Pt(CN)_4Br_2]_\infty \cdot 10/3(H_2O)$ (**1**) were collected by filtration. (Yield 507 mg, 0.83 mmol, 83 %)

Synthesis of 2

To 5 ml of aqueous solution of K_2PtCl_4 415 mg (1.00 mmol) was added KCN 260 mg (4.00 mmol) and stirred until the solution became colorless. $AgNO_3$ 679 mg (4.00 mmol) was added and stirred ca. 24 h under dark. The precipitate (AgCl) was filtered off by celite filtration. Approximately 250 mg (~1.5 eq) of Br_2 was added and stirred for 30 min, and then heated to 50 °C for another 30 min to remove excess of Br_2 in the solution. After cooling, to the solution was added 5 ml of 0.2 M aqueous solution of $NiBr_2 \cdot 3H_2O$ and stand overnight. Obtained yellow color crystals of $[Ni(H_2O)_2Pt(CN)_4Br_2]_\infty \cdot 8/3(H_2O)$ (**2**) were collected by filtration. (Yield 534 mg, 0.89 mmol, 89%)

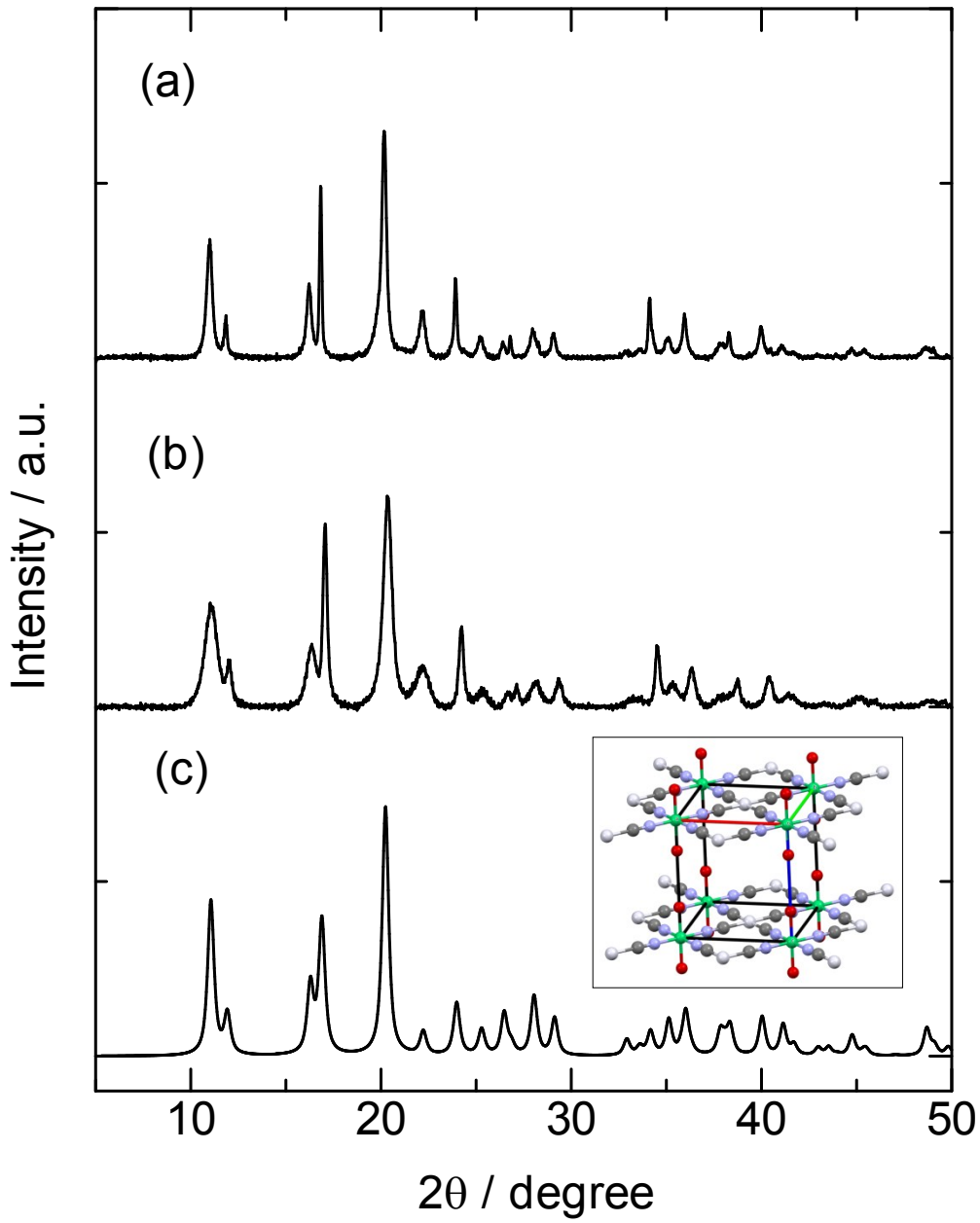

Fig. S1 Experimental PXRD patterns of Hofmann clathrate synthesized by mixing 0.2 M aquesous $K_2Pt(CN)_4$ and 0.2 M $Co(NO_3)_2$ (a) or $NiBr_2$ (b), respectively. The PXRD patterns was well indexed by assuimg the following parameters, Tetragonal, a = 7.41 Å, c = 7.99 Å for (a) and Tetragonal, a = 7.33 Å, c = 8.00 Å for (b), by using DASH software containing in the CSD software package. Fig. 1(c) shows the PXRD pattern simulated from the crystal structure shown in the inset of Fig. 1(c). Color code; White: Pt, Gray: C, Blue: N, Green, Ni. Red: O.

Table S1 Crystallographic data of **1** (rt and 70 °C)and **2** (rt)

	1 (rt)	**1** (70 °C)	**2** (rt)
Empirical Formula	$C_4Br_2Co_1N_4O_{5.33}Pt_1$	$C_{12}Br_6Co_3N_{12}O_{14}Pt_3$	$C_{12}Br_6N_{12}Ni_3O_{14}Pt_3$
Formula weight	603.17	1777.67	1176.95
Crystal system	Trigonal	Cubic	Cubic
Space group	*R*-3m	*Pm*-3*m*	*Pm*-3*m*
Crystal size (mm^3)	0.20×0.20×0.20	0.20×0.20×0.20	0.20×0.20×0.20
a (Å)	14.997(3)	10.4037(8)	10.338(9)
c (Å)	17.444(3)	–	–
V ($Å^3$)	3397.6(17)	1126.1(3)	1105(3)
Z	9	1	1
T (K)	293(2)	343(2)	293(2)
μ (mm^{-1})	15.652	15.741	16.197
ρ_{calcd}	2.607	2.612	2.695
F(000)	2379	793	804
GOF on F^2	1.170	1.140	1.115
R_1, wR_2 [I > 2σ]	0.0376, 0.0818	0.0199, 0.0530	0.0292, 0.0646
R_1, wR_2 [all data]	0.0395, 0.0824	0.0209, 0.0537	0.0347, 0.0662
Reflns. measured	1389	340	326
CCDC No.	1503125	1503126	1503124

Table S2 Experimental and calculated data of elemental analyses

	C	H	N	Br	Co	Ni	Pt
found for **1**	8.007	1.757	9.135	25.84	9.47	-	31.67
calcd. for $C_4H_{10.67}Br_2Co_1N_4O_{5.33}Pt_1$	7.83	1.75	9.13	26.03	9.60	-	31.77
found for **1''**	9.786	3.251	11.075	0.74			
calcd. for $C_4H_{16}Co_1N_4O_8Pt_1$	9.57	3.21	11.16	0.00			
found for **2**	7.983	1.916	8.964	25.49	-	9.43	32.29
calcd. for $C_4H_{9.33}Br_2Ni_1N_4O_{4.67}Pt_1$	7.98	1.56	9.31	26.56	-	9.75	32.42
found for **2''**	10.142	2.642	11.278	0.97			
calcd. for $C_4H_{14}Co_1N_4O_7Pt_1$	9.93	2.92	11.58	0.00			

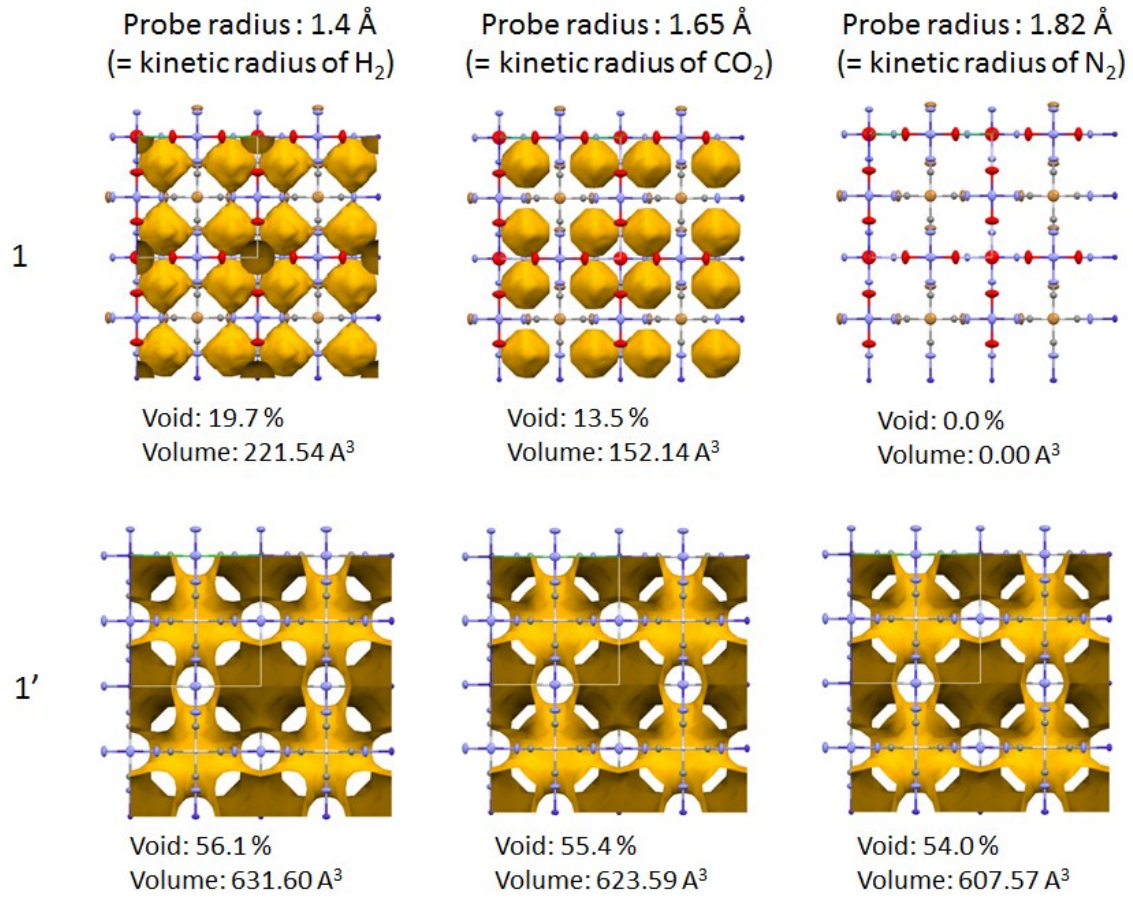

Fig. S2 Calculated void space of **1** (upper) and **1'** (lower) with a probe radii of 1.4 Å(left), 1.65 Å(middle), and 1.82 Å(right), respectively.

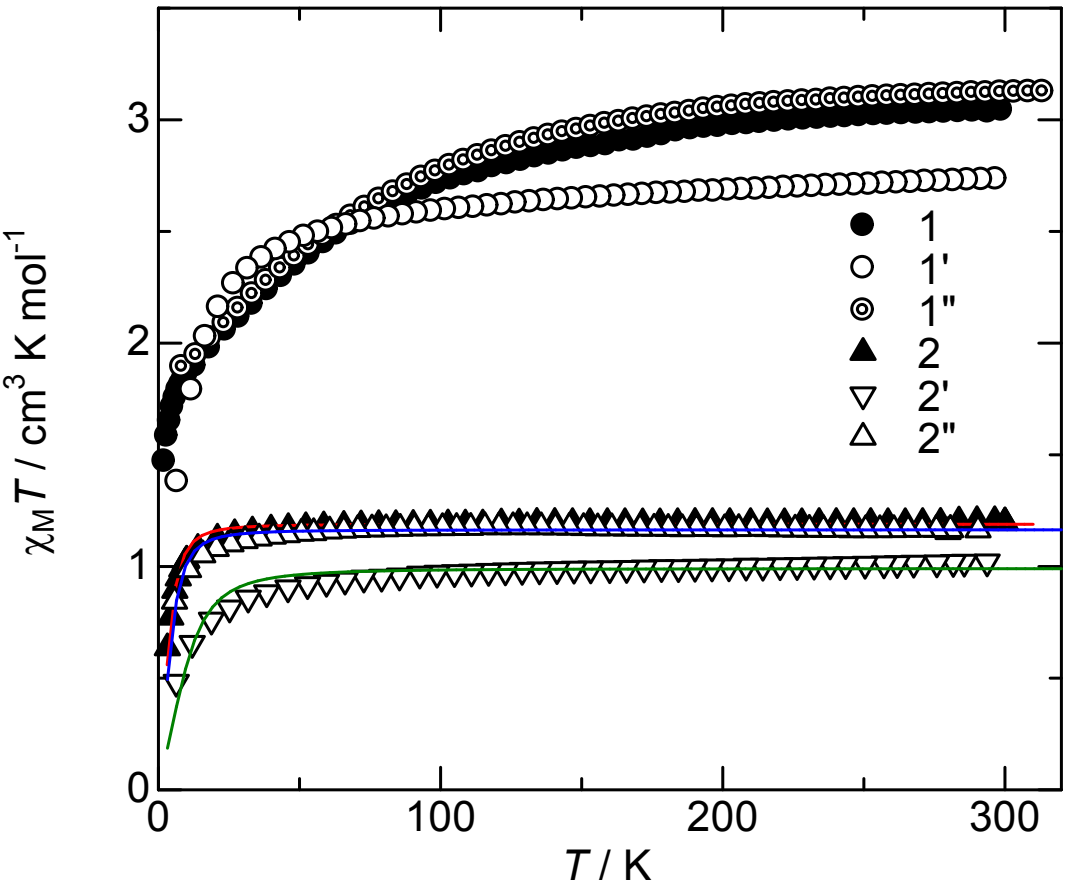

Fig. S3 Magnetic susceptibility of **1, 1‘, 1“, 2, 2‘** and **2“** under 1000 Oe.

Discussion about the magnetic susceptibility

The magnetic susceptibilities of **2**, **2'** and **2"** were fitted by $S = 1$ van Vleck's equation as follws,[S1]

$$\chi_{iso} = \frac{2Ng^2\mu_B{}^2}{3kT}\left[\frac{2kT/D - \frac{2kTexp(-D/kT)}{D} + exp(-D/kT)}{1 + 2exp(-D/kT)}\right]$$

where N, μ_B and k represent Avogadro constant, Bohr magneton and Boltzmann constant, respectively. The best fit parameters are $g = 2.18$ and $D = +13.1$ K for **2** (red curve), $g = 1.99$ and $D = +34.2$ K for **2'** (green curve), and $g = 2.16$ and $D = +15.0$ K for **2"** (blue curve). For **1**, **1'**, and **1"**, no modeling was conducted due to overparametrization. The magnetic susceptibility of **1** and **1"** (**2** and **2"**) are mostly identical, suggesting that Co (Ni) ion is in the same coordination geometry. On the other hand, the susceptibility of **1'** and **2'** is different from those of **1** and **2**, respectiliby, indicating that the local coordination environment chaged by the removal of the axial water molecules.

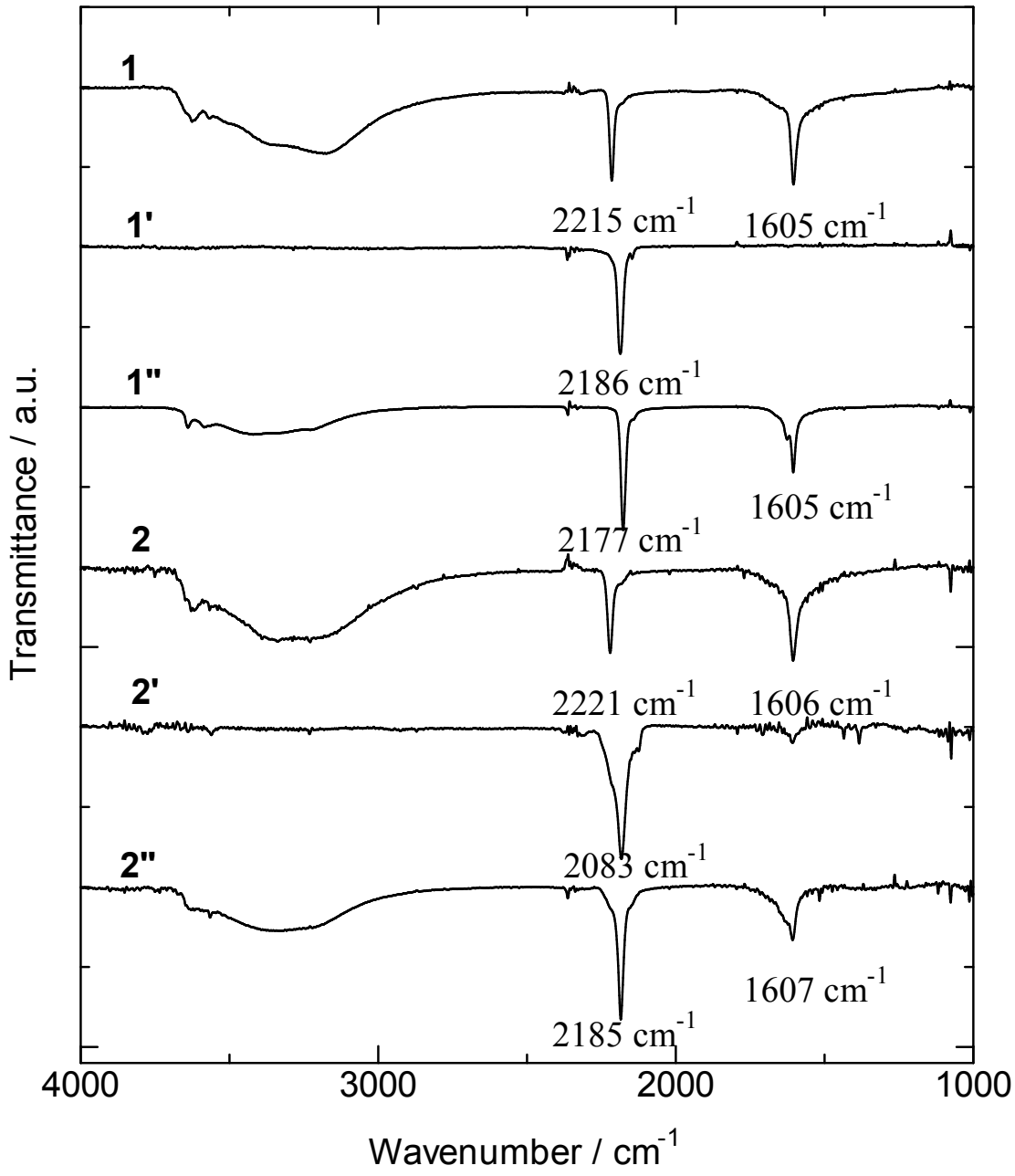

Fig. S4 FT-IR spectra of **1**, **1‘**, **1“**, **2, 2‘** and **2“**.

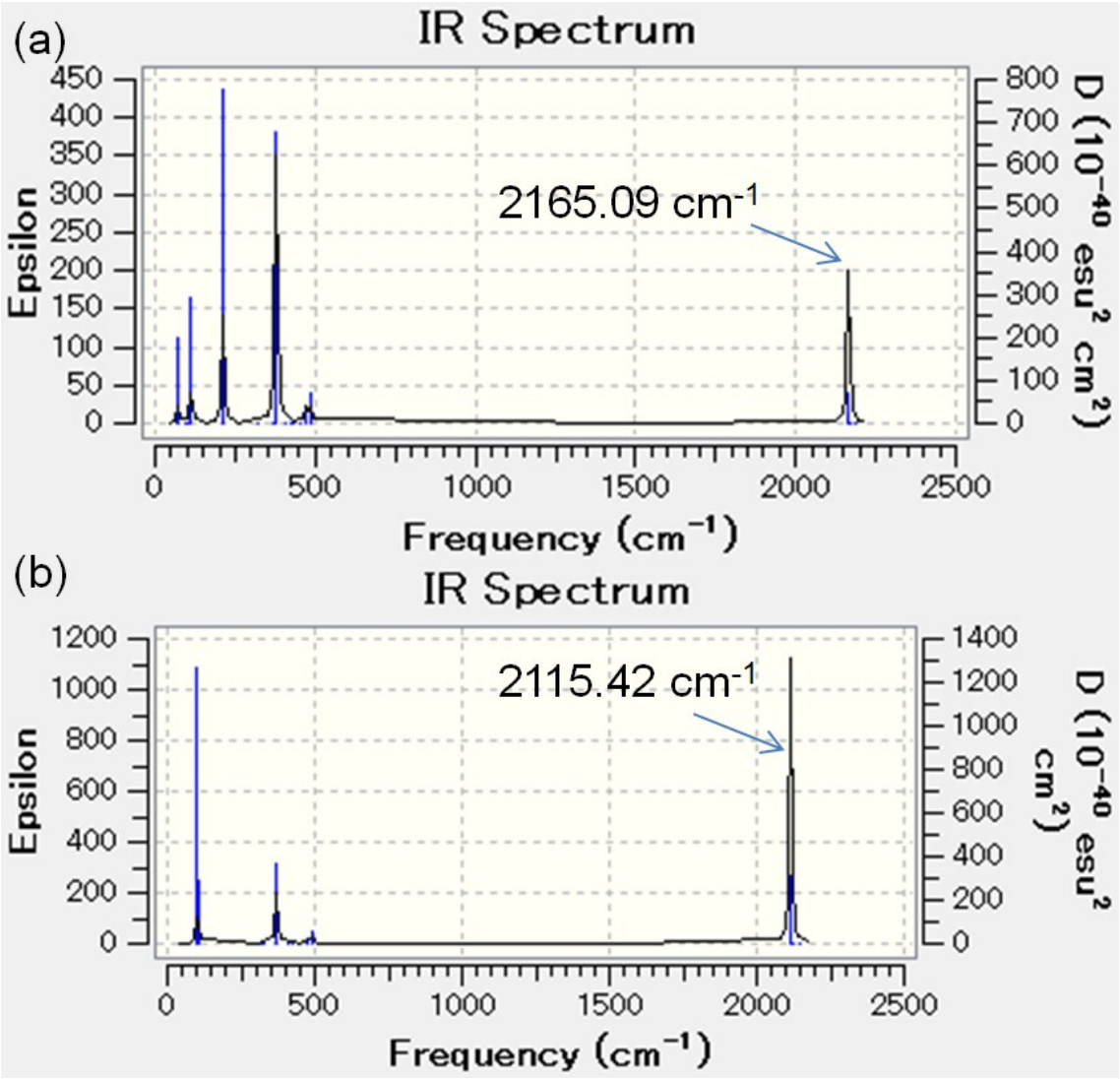

Fig S5 Calculated IR spectra of (a) $[Pt(CN)_4Br_2]^{2-}$ and (b) $[Pt(CN)_4Br_2]^{2-}$. For the DFT calulation, structural optimization was performed before frequency caluculation with LANL2DZ basis set. The peaks 2165.09 and 2115.42 cm^{-1} is asigned to CN stretching mode.

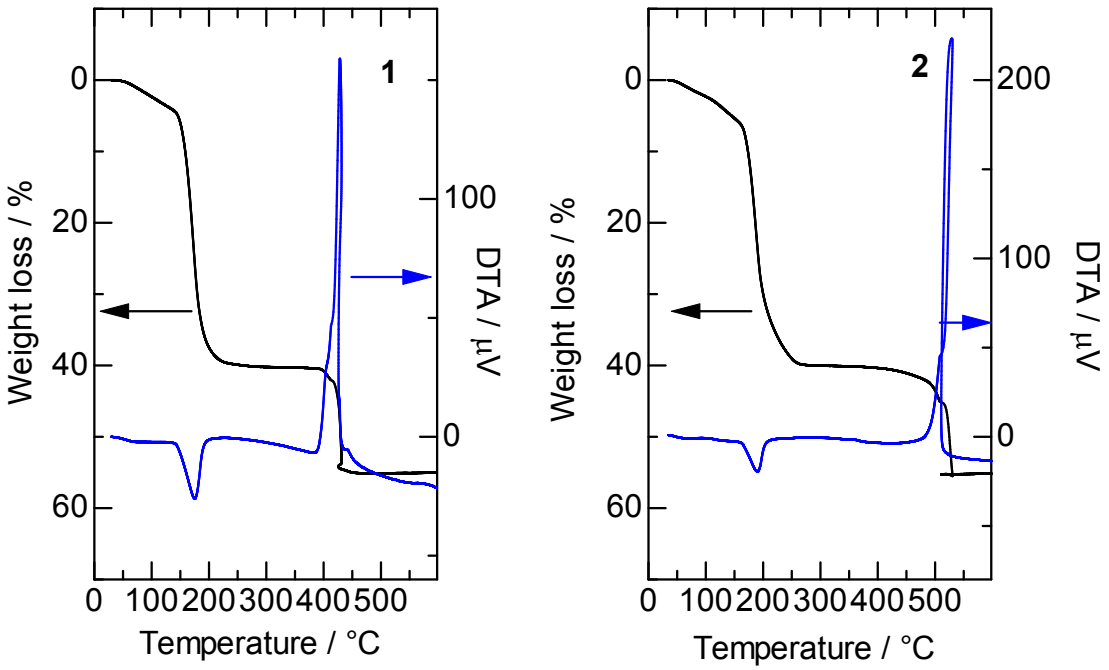

Fig. S6 TG/DTA of **1** and **2** up to 600°C (5°C/min) under arerobic condition. The exothermic wight loss at around 400 °C and 500 °C in **1** and **2**, respectively, corresponds to the thermal decomposition. The final product was a mixture of Pt and Co_3O_4 in the case of **1** and NiO in the case of **2**, confirmed by using powder X-ray diffraction (PXRD) patterns of the decomposed compounds (Fig. S7).

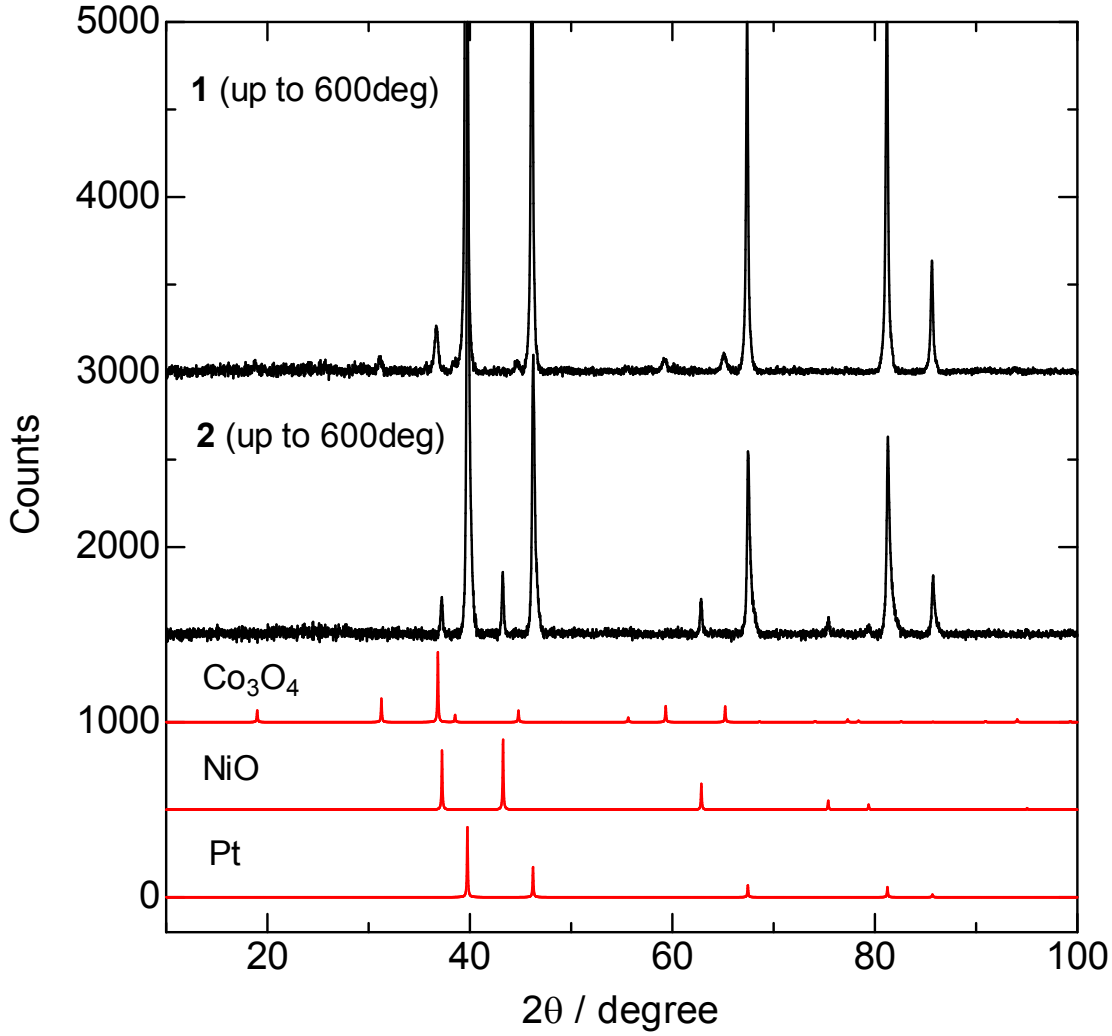

Fig. S7 PXRD patterns of **1** and **2** after heating up to 600°C in air together with simulated patterns of Pt, Co_3O_4 and NiO for comparison.

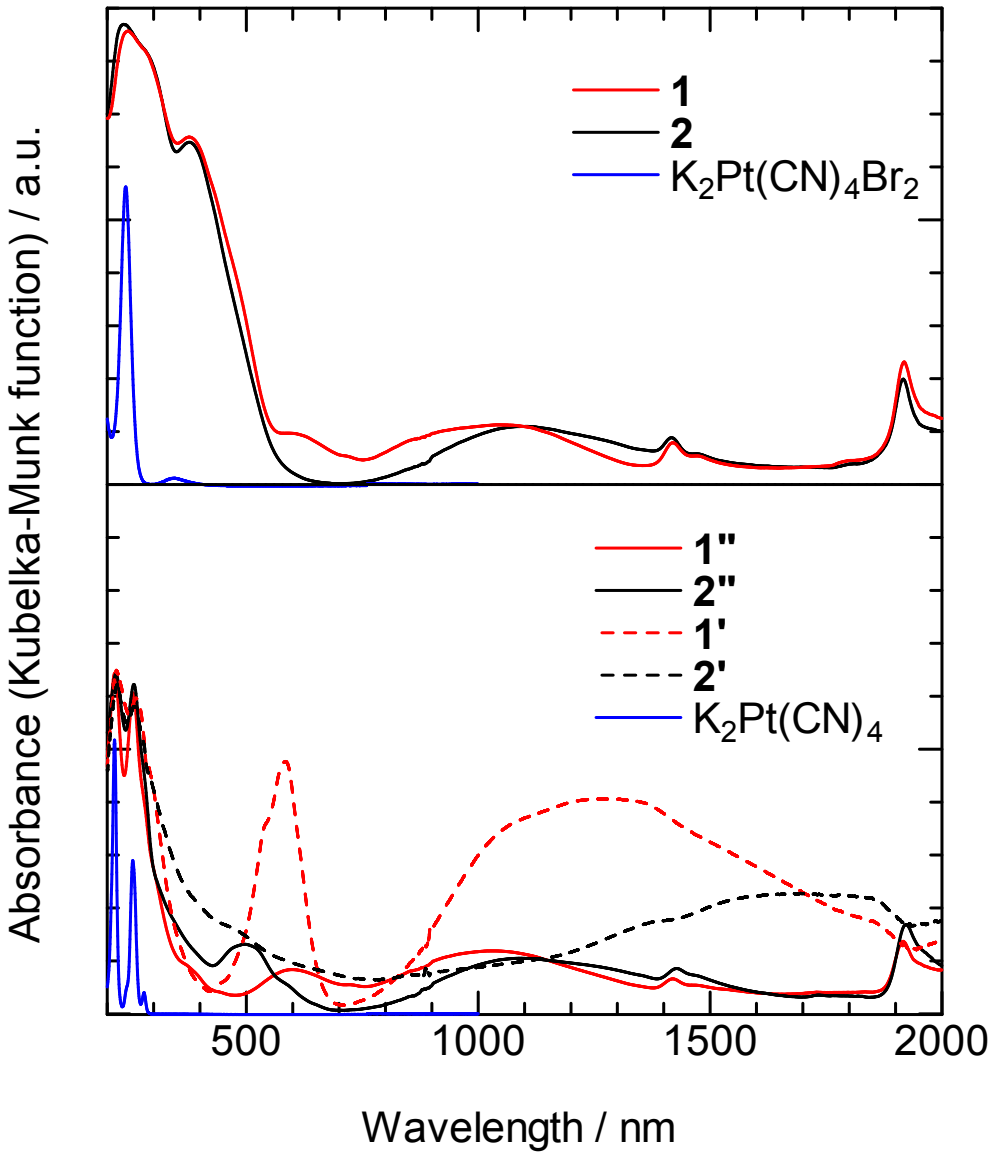

Fig. S8 UV-vis-NIR spectra of **1**, **1‘**, **1“**, **2**, **2‘** and **2“** together with those of aqueous solution of $K_2Pt(CN)_4Br_2$ and $K_2Pt(CN)_4$.

Discussion about UV-vis-NIR spectra

Comparing the spectra of **1**, **1‘**, **1“**, **2**, **2‘**, and **2“** as well as those of aqueous $K_2Pt(CN)_4$ and $K_2Pt(CN)_4Br_2$, the intense peaks at the UV ($\lambda < 400$nm) region can be attributable to Pt spiecies because the spectrum shape depends on the oxidation state of Pt center and independent of M‘ (M‘ = Co or Ni). Thus, we have normalize the absorbance of the compounds by using peak hights of them in UV region. On the other hand, the peaks in the vis-NIR region (400nm $< \lambda <$ 1500 nm) can be assined to d-d transition of M‘ ions because no prominent peak was observed in the aqueous solution of $K_2Pt(CN)_4$ and $K_2Pt(CN)_4Br_2$. **1** and **1“** (or **2** and **2“**) showed quite similar spectra at vis-NIR region, reflecting the similar coordination environment of M‘ ions between them. The spectra of **1‘** and **2‘** is similar with those of **1“** and **2“** in the UV region, respectively, whereas quite different in the vis-NIR region, which can be explained by the diffrence in the local coordination environment of M‘ ions. The larger absorbance in **1‘** than **1** or **1“** should be due to the relaxation of Laporte rule in the tetrahedral geometry.

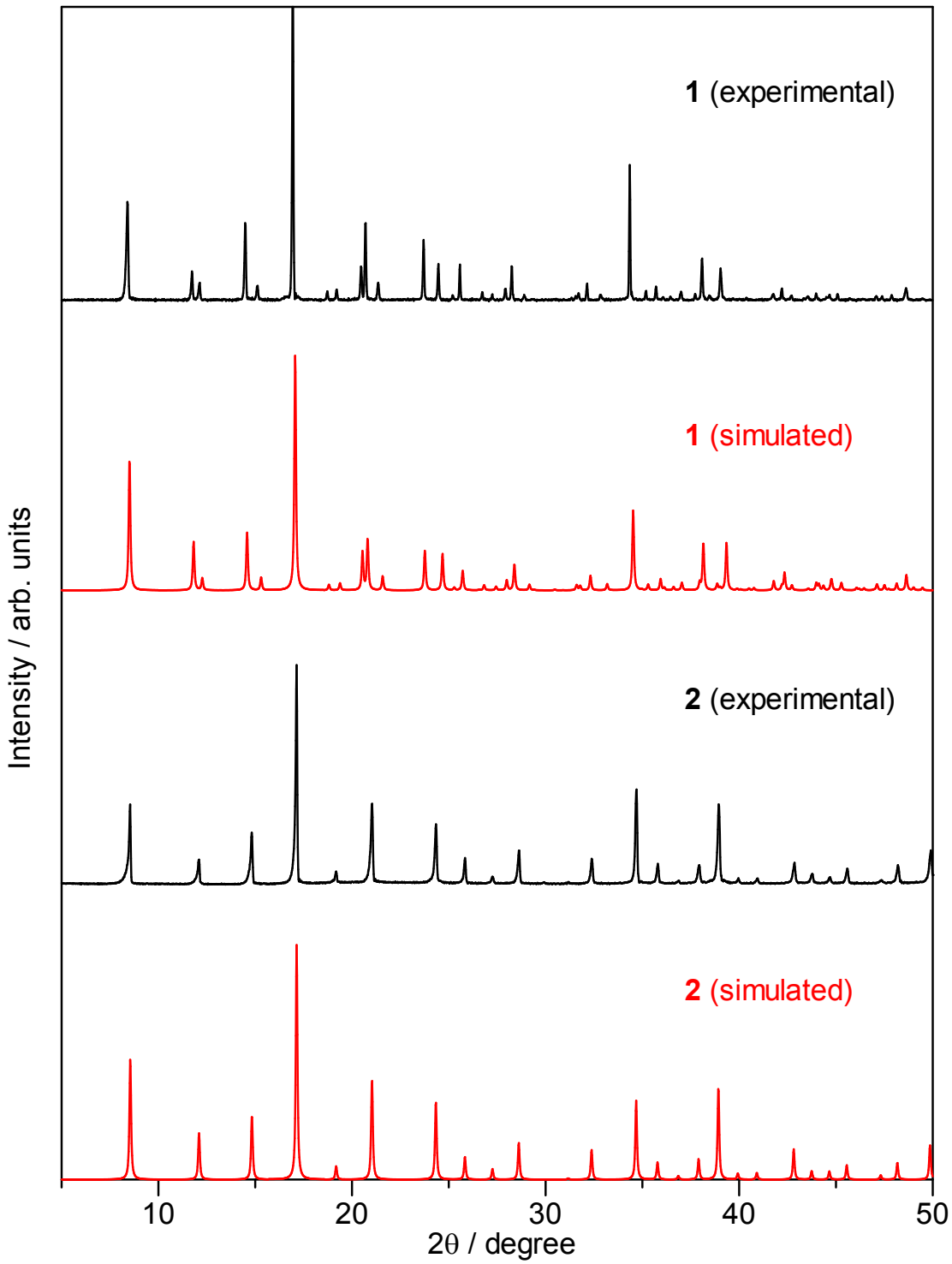

Fig. S9 Simulated and experimental PXRD patterns of **1** and **2** at room temperature.

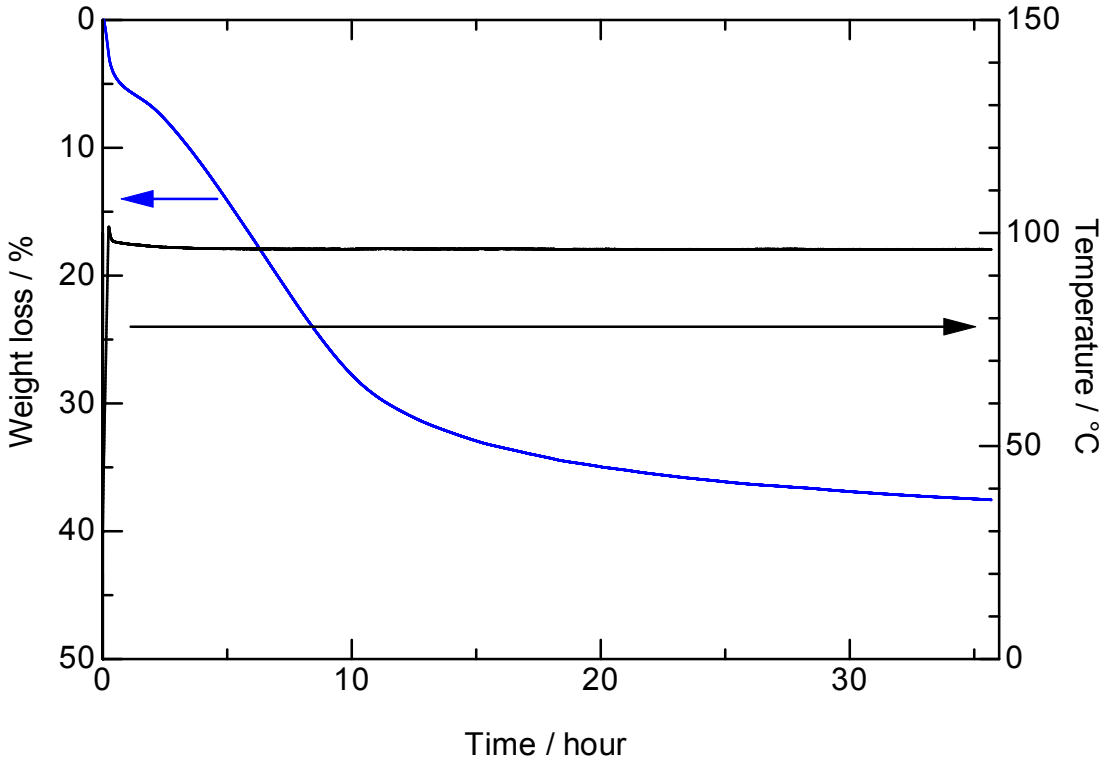

Fig. S10. Time evolution of the wight loss in **1** at 100°C under N_2 atmosphere.

Discussion about the local coordination environment of anhydrous 1‘ and 2‘

Here we discuss the local coordination environment of **1‘** (M‘ = Co) and **2‘** (M‘ = Ni). For **2‘**, PXRD pattern did not changed except for the peak intensity by removing axial water molecules, indicating that the MOF skelton does not changed. Thus, we can simply conclude that Ni ion in **2‘** have a square planer geometry. This is also supported by the finding that the yellow color of **2‘** is typical in the sqare planer Ni^{2+} complexes.

On the other hand, consideration of the local environment of **1‘** is not straightforward because of significant change in the PXRD pattern as well as lost of long range lattice ordering by removing axial water molecules. However, FT-IR spectrum of **1‘** showed a clear single peak at 2186 cm^{-1} (Fig. S4), suggesting that **1‘** has a uniform local structure. In addition, UV-vis spectrum showed much larger absorbance was observed. This suggests that relaxation of Laporte‘s selection rule, which usually occurs by d-p hybridization in the tetrahedral geometry. Especially, the peak at 585 nm with a shoulder peak at 540 nm (right fig.) is quite similar with the UV-vis spectrum of $Co[Au(CN)_2]_2$ with a tetrahedral coordination geometry (590 nm, 550 nm(sh)).[S2] Thus, we estimated that Co ion is in tetrahedral coordination geometry. Transformation from square planer to tetrahedral geometry in the framework should accompanied by the Co-N bond cleavage and reformation, causing poor crystallinity of **1‘**.

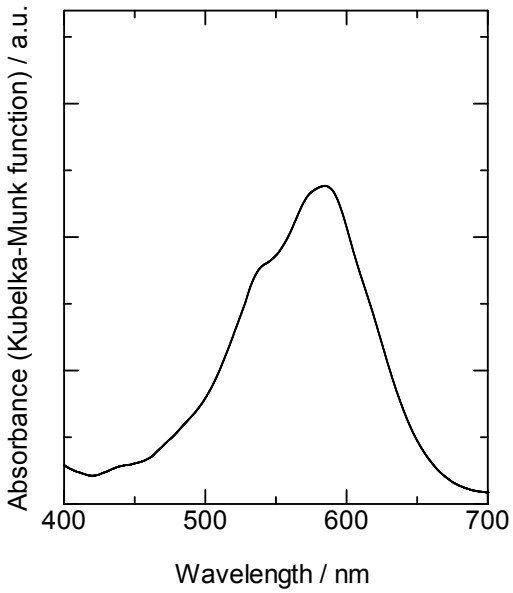

Reference

S1 R. L. Carlin, Magnetochemistry, Springer-Verlag, Berlin Heiderberg New York Tokyo, 1985, pp.24.

S2 J. Lefebvre, J. L. Korcok, M. J. Katz D. B. Leznoff, *Sensors,* 2012, **12**, 3669-3692.